ACS APPLIED MATERIALS & INTERFACES

Research Article

www.acsami.org

Tuning Surface Mechanical Properties by Amplified Polyelectrolyte Self-Assembly: Where "Grafting-from" Meets "Grafting-to"

Ang Li,[†] Shivaprakash N. Ramakrishna,[†] Tobias Schwarz,[‡] Edmondo M. Benetti,[†,§] and Nicholas D. Spencer*[,†]

[†]Laboratory for Surface Science and Technology, Department of Materials, ETH Zurich, Wolfgang-Pauli-Strasse 10, 8093 Zurich, Switzerland

[‡]Light Microscopy and Screening Center, Department of Biology, ETH Zurich, Schafmattstrasse 18, 8093 Zurich, Switzerland

[§]Department of Materials Science and Technology of Polymers, University of Twente, MESA+ Institute for Nanotechnology, P.O. Box 217, 7500 AE Enschede, The Netherlands

Supporting Information

ABSTRACT: We report the interaction of surface-tethered weak polyacid brushes, poly(methacrylic acid), with a weak polybase poly(L-lysine)-*graft*-poly(ethylene glycol), in solution. The grafted polyacid brushes, grown directly from the silicon substrate by UVLED surface-initiated polymerization, act as a nanotemplate for the solution-phase polybase, which penetrates into the brushes, forming a polyelectrolyte complex (PEC), whose mechanical and nanotribological properties are markedly influenced by the electrostatic assembly conditions. The mechanical effects are amplified due to the architecture of the specific polybase used, which contributes approximately 2k Da per unit charge to the overall system, resulting in an efficient filling of the polyacid brushes, which thus acts as a scaffold. The distribution of the adsorbed copolymers in the PEC films has been investigated by means of confocal microscopy. The unique structure of the PEC films provides a system whose mechanical and nanotribological properties can be tuned over a wide range.

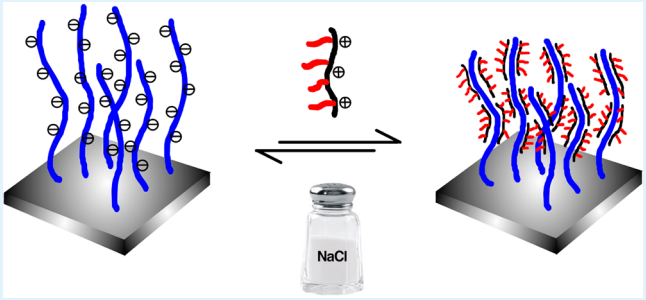

KEYWORDS: *polymer brushes, polyelectrolyte assembly, 'grafting-from', mechanical properties, aqueous tribology, polymer coatings*

INTRODUCTION

Surface modification (of organics, inorganics, and metals) by adhering polymer species with well-defined structures, is a highly desirable approach to tailoring interfacial properties for specific applications. To this end, different fabrication strategies have been proposed during the last two decades. As two major examples, both the controlled grafting of polymer chains (either adsorbed from solution or grown from the substrate to form polymer brushes)/gels[1−6] and the fabrication of polymer multilayers[7] have been extensively investigated. The former approach involves tethering polymer chain ends at interfaces, whereas the latter method features the layer-by-layer (LbL) assembly of oppositely charged macromolecules. These fabricated thin films show well-defined architectures and have been applied to the modification of biomaterials or, alternatively, for the fabrication of three-dimensional nano-objects for drug delivery or advanced sensing devices (e.g., nanoparticles, quantum dots).[8−12]

An emerging surface-modification strategy that combines the two approaches of surface grafting and charge-based assembly is the so-called polyelectrolyte self-assembly, where grafted polyelectrolytes act as receptors for oppositely charged polymer chains that adsorb from solution, into the grafted polyelectrolyte layer. This approach has been shown to enhance the control over the films' composition and thickness to nanometer precision. In this context of integrating "grafting-from", "grafting-to" and LbL techniques, Rühe et al. pioneered the methodology by assembling poly(4-vinyl-*N*-methylpyridinium) iodide into poly(methacrylic acid) (PMAA) brushes. The generated films were thus composed of surface-attached polyelectrolyte complexes (PECs), and displayed film thicknesses ranging from a few to several tens of nanometers, and could act as starting platforms for polyelectrolyte multilayers.[13]

Moya et al. additionally exploited similar PEC films for templating 3D structures featuring hollow patterns and ledges on the nanoscale, and demonstrated the possibility of fabricating extended architectures, using a grafted polymer layer as a scaffold.[14] The characteristics of the grafted layer (i.e., grafting density or chain length) have been shown to influence the assembly of polyelectrolyte from solution, which in turn determines the properties of the subsequently fabricated multilayered films, as reported by Portinha and Charlot.[15]

Inspired by these preliminary reports, our study focuses on the fabrication of grafted PEC films by the electrostatic-driven

Received: February 21, 2013
Accepted: May 8, 2013
Published: May 8, 2013

   dx.doi.org/10.1021/am4006379 | ACS Appl. Mater. Interfaces 2013, 5, 4913−4920

assembly of poly(L-lysine)-*graft*-poly(ethylene glycol) (PLL-*g*-PEG) into poly(methacrylic acid) (PMAA) brushes, that had been previously grafted from 2D surfaces. Graft copolymers with a positively charged PLL backbone and PEG side chains have been reported to form ultrathin films and act as widely applicable surface modifiers for a variety of negatively charged surfaces (ranging from glass to titania) and have shown excellent biopassive and lubricating properties.[16,17] In this study we assembled PLL-*g*-PEG species into PMAA grafts to form PEC films and this self-assembly mechanism was studied under a range of conditions. The generated PEC films presented variable thicknesses depending on the assembly conditions, which ranged from a few tens to several hundred nanometers. The mechanical and nanotribological properties varied noticeably from the pristine PMAA brushes to the saturated grafted PEC films. Furthermore, the PEC films demonstrated fully reversible characteristics following salt-driven desorption of PLL-*g*-PEG adsorbents from the brush scaffolds. The morphologies and structures of these films were further investigated by using atomic force microscopy (AFM) and confocal fluorescence microscopy, in order to gain additional insights into the architecture of the films.

We propose a general approach to generating grafted PEC films with controlled thickness, presenting variable and reversible interfacial and mechanical properties. These effects can be amplified by the use of polybase architectures that have an intrinsically high mass per unit charge. Grafted PECs show promise for further application in the fabrication of multifunctional, quasi-3D structures, which may find a wide range of technologies ranging from the tailoring of biomaterial interfaces, to the development sensing platforms and the fabrication of intelligent membranes.

EXPERIMENTAL SECTION

Materials. *p*-(Chloromethyl)phenyltrimethoxysilane (ABCR, Germany), PLL(20k)-*g*(3.3)-PEG(5k) (SuSoS AG, Dübendorf, Switzerland), PLL(20k)-*g*(3.3)-PEG(2k)/TRITC (fluorescent red label, TRITC labeling approximately 4%, emission wavelength max 625 nm, SuSoS AG, Dübendorf, Switzerland), PLL(20k)-*g*(3.3)-PEG(2k)/FITC (fluorescent green label, FITC labeling approximately 4%, emission wavelength max 514 nm, SuSoS AG, Dübendorf, Switzerland), methanol (Fluka, Switzerland), triethylamine (>99.5%, Sigma-Aldrich, Switzerland), sulfuric acid (95−97%, Sigma-Aldrich, Germany), and hydrogen peroxide (30 wt % in water, Merck, Germany) were all used as received. Tetrahydrofuran (99.5% extra dry, Acros, Germany) and toluene (>99.7%, Fluka-Chemie AG, Switzerland) were freshly distilled over sodium prior to use. Methacrylic acid (98%, Fluka-Chemie AG, Switzerland) was first passed through an inhibitor-remover column (Sigma-Aldrich, Switzerland) and subsequently distilled under vacuum. Sodium *N*,*N*-diethyldithiocarbamate (97%, Fluka, Switzerland) was recrystallized from methanol. Water was deionized with a GenPure filtration system (18.2 MΩ cm, TKA, Switzerland). HEPES buffer was prepared by dissolving 1 mM 4-(2-hydroxyethyl)-1-piperazineethanesulfonic acid (HEPES, BioChemika Ultra, Fluka, Switzerland) in Milli-Q water, and adjusting the solution pH to 7.4.

Synthesis and Characterization of PMAA Brushes and PEC Films. PMAA brushes were first synthesized from silicon oxide substrates by means of UV-LED iniferter-mediated surface-initiated polymerization (UVLED-SIP). The synthesis of the silane-based iniferter and its surface immobilization were performed according to the reported procedures.[18] UVLED-SIP proved to provide fast, catalyst-free, and well-controlled grafting of polymer brushes.

Subsequent fabrication of grafted PEC films was carried out by dipping prewetted PMAA brush samples (1 cm × 0.5 cm) into PLL-*g*-PEG solutions at various concentrations and for different incubation times. Following the formation of PEC films, samples were extensively rinsed with Milli-Q water and further incubated in Milli-Q water overnight, in order to remove any loosely adsorbed polymer chains prior to characterization.

The dry thicknesses of both PMAA brushes and grafted PEC films were determined by means of a variable-angle spectroscopic ellipsometer (VASE) (M-2000F, LOT Oriel GmbH, Darmstadt, Germany) at three different incidence angles (65, 70, 75°), in ambient environments with a relative humidity of 28.4%, under the assumption that the polymer has a refractive index of 1.45. The thickness was determined via the analysis of a five-layer (Si/SiO_2/iniferter/PMAA (or PEC)/Ambient) model with known thicknesses and refractive indices of the Si, SiO_2 and iniferter layers (software WVASE32, LOT Oriel GmbH, Darmstadt, Germany). FT-IR spectra were recorded on the dried samples in transmission mode by employing an infrared spectrometer (Bruker, IFS 66 V) equipped with a liquid-nitrogen-cooled MCT detector. A background spectrum was collected from a freshly cleaned, bare silicon wafer.

The morphologies of PMAA brushes and grafted PEC films in a dry state were measured by a Dimension AFM with a NanoScope IIIa controller (Digital Instruments, Santa Barbara CA) in tapping mode with a silicon cantilever (Olympus, Japan) with a resonant frequency of 300 kHz and a spring constant of 26.1 N/m (manufacturer values).

Confocal Fluorescence Microscopy. z-Stacks were acquired with a Zeiss LSM 780 equipped with a GaAsP detector and a LD C-Apochromat 40×/1.1 W Korr M27 objective. A DPSS 561 nm laser was used for TRITC excitation (red), and a 488 nm Argon laser line for FITC excitation (green). The pinhole was set to 10 μm and *z*-stacks were acquired at an interval of 0.2 μm. Images were visualized and processed with Imaris (Version 7.5.2, Bitplane). Mean fluorescence intensities were determined using ImageJ software (National Institutes of Health, USA).

Colloidal Probe Microscopy. Normal-force and friction measurements between a gold-coated silica microsphere and PMAA brushes or grafted PEC films with different adsorbed amounts of PLL-*g*-PEG were carried out in HEPES buffer using an AFM (MFP3D, Asylum Research, Santa Barbara, USA) equipped with a liquid cell. The normal spring constant of the Au-coated tipless cantilever (NSC-12, Mikromash, Estonia) was measured by the thermal-noise method[19] and the torsional spring constant was measured according to Sader's method.[20] Both normal and torsional spring constants of the cantilever were measured before attaching the colloidal microsphere. A silica microparticle (EKA chemicals AB, Kromasil) was glued with UV-curable glue (Norland optical adhesive 63) to the end of the tipless cantilever by means of a home-built micromanipulator, to be further used for colloidal probe microscopy.[21] The probe was coated with 2 nm of chromium and subsequently 10 nm of gold using an evaporator (MED020 coating system, BAL-TEC, Balzers, Lichtenstein).

The lateral-force calibration was conducted by employing the "test-probe method".[22] To determine the lateral sensitivity of the photo detector, a freshly cleaned silicon wafer (1 cm ×1 cm) was glued "edge-on" to a glass slide. The smooth silicon plane was used as a "wall" for measuring the lateral sensitivity. A test probe (cantilever glued with a silica colloidal sphere of diameter around 40 μm) was moved laterally into contact. The slope of the obtained lateral-deflection-vs-piezo-displacement curve yields the lateral sensitivity, to be used for lateral-force calibration.

For lateral-force measurements, 10 "friction loops" along the same scan were acquired at each load (scanning rate, 1.0 Hz; stroke length, 5.0 μm), from which the average friction force and the standard deviation were calculated. Both normal-force and friction measurements were repeated at three different locations on the polymer films.

The apparent elastic moduli of the polymer films were estimated from the nanoindentation curves using the Hertz model as described elsewhere[23]

$$F = \frac{4\sqrt{r_{tip}}}{3(1-\nu^2)} E\delta^{1.5} \quad (1)$$

$$F = kd \quad (2)$$

$$\delta = z - d \quad (3)$$

where F is the applied load, r_{tip} is the radius of the colloidal probe, ν is the Poisson's ratio of the polymer films (assumed to be 0.5), E is the apparent Young's modulus of polymer films, δ is the deformation of the polymer films (calculated from the relative piezo-extension z and relative deflection of the cantilever d), and k is the spring constant of the cantilever.

A constant applied force with an indenting speed of 3.97 μm/s was employed during the indentation measurements. The initial 10% of the approach curve was used to measure the Young's modulus of the polymer films, in order to avoid a substrate effect on the measured values. By fitting the force curves (based on 16 individual measurements) acquired during normal-force measurements into eqs 1−3, one can obtain the apparent Young's modulus of the polymer films E.

RESULTS AND DISCUSSION

Adsorption Kinetics of Grafted PEC Films. The adsorption behavior of PLL-*g*-PEG in PMAA brush platforms of different film thicknesses (chain lengths) was studied by VASE and is compared to the adsorption behavior of PLL-*g*-PEG on bare silicon oxide (Scheme 1 and Figure 1). In the latter case, graft copolymers showed an initial fast adsorption, followed by a slowing down of the film growth rate (inset in Figure 1). Fast adsorption kinetics occurs initially because of the electrostatic interactions between the positively charged PLL moieties and the negatively charged silicon oxide surface. After attaining an initial coverage, the adsorption rate gradually decreases, owing to the high concentration of polymer chains at the surface leading to steric hindrance that further inhibits assembly. A saturation film thickness of 1.2 ± 0.1 nm was finally reached after 30 min of incubation.[24]

Scheme 1. (a) "Grafting to" of PLL-*g*-PEG onto a Silicon Wafer and (b) "Grafting to" of PLL-*g*-PEG into Surface-Grafted PMAA Brushes (proposed structure for polyelectrolyte complex films)

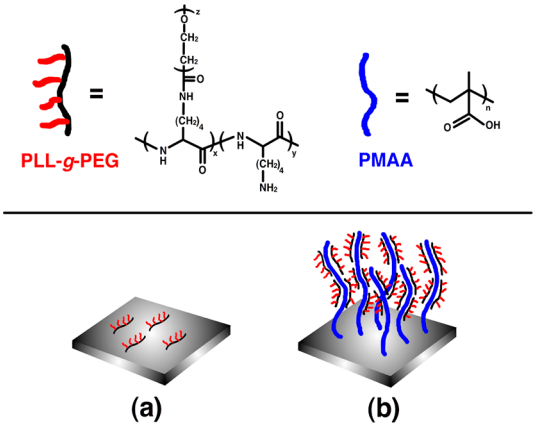

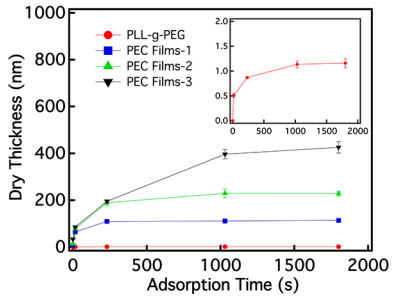

Figure 1. Adsorption kinetics of PLL-*g*-PEG (2.5 mg/mL in HEPES buffer with a pH of 7.4) on a silicon wafer (inset) and on PMAA brushes, as a function of adsorption time. Initial dry thicknesses of PMAA brushes for preparing PEC films 1, 2, and 3 were 7, 13, and 33 nm, respectively.

The mass of PLL-*g*-PEG adsorbed into the PMAA brush layer was found to be two orders higher in magnitude than that of PLL-*g*-PEG adsorbed onto bare silicon oxide samples. Yet the adsorption profiles of PLL-*g*-PEG into PMAA brushes, starting with different PMAA dry thicknesses (namely 7, 13, and 33 nm as shown in Figure 1), followed similar kinetics: initial fast adsorption and a subsequent slowing down of the adsorption rate until a plateau was reached (Figure 1).

A 30 min adsorption of PLL-*g*-PEG increases the dry thickness of PEC films to 100, 200, and 500 nm (obtaining PEC films-1, PEC films-2, and PEC films-3, respectively) from 7, 13, and 33 nm of PMAA brushes, respectively. Thus the dry height of the PECs is comparable to the wet height of the PMAA brushes,[25] suggesting that the PLL-*g*-PEG is essentially filling the space within the brushes.

In addition, it should be mentioned that the saturation time for achieving the maximum thickness of PEC films also increased with the starting thickness of PMAA brushes. This observation suggests an adsorption mechanism involving complexation of the graft copolymers into the brush architecture, which becomes more difficult in longer brushes because of the increased diffusion lengths involved, prior to encountering free charges.

The driving force for fabricating the PEC films is the formation of the water-soluble weak polyelectrolyte complex between oppositely charged PMAA brushes and PLL-*g*-PEG. As pointed out by de Vos,[26] anchoring weak polyacids on silicon substrates enables the creation of a significant volumetric charge density. In this case, the thickness of the grafted PEC films is tunable by either varying the starting thickness of the PMAA brushes or by changing the PLL-*g*-PEG adsorption time. During the initial (fast) adsorption, PLL-*g*-PEG with a relatively small molecular size (apparent contour length of 53 nm, apparent persistence length of 19.9 nm and radius of gyration equal to 12.2 nm)[27] rapidly diffused into the highly swollen PMAA brushes (characterized by an average swelling ratio of 26)[25] and complexed with the PMAA backbones. Further adsorption of PLL-*g*-PEG was progressively hindered by the physical barrier of the newly formed PEC layer, which slowed down adsorption and complexation of additional PLL-*g*-PEG. As a result, a thickness saturation was reached (plateaus in the adsorption profiles in Figure 1).[28]

PLL-*g*-PEG loading within the PMAA brush structure was also studied by FT-IR composition analysis (see the Supporting Information). Prior to adsorption of the graft copolymers, O−H (3200 cm^{-1}), C−H (3000 cm^{-1}) and C═O stretching (1710 cm^{-1}) vibrations, representative of PMAA films, could be clearly identified.[29] Following the complexation of PLL-*g*-PEG into the PMAA matrix, these characteristic peaks were overshadowed by the characteristic signals of PEG segments i.e. C−H (2890 cm^{-1}) and C−O stretching (1110 cm^{-1}).[30]

The amount of complexed PLL-*g*-PEG and the subsequent thickness of grafted PEC films were also studied as a function of the concentration of adsorbing copolymer, at constant adsorption time. As shown in Figure 2, the thickness of the grafted PEC films was found to be linearly proportional to the PLL-*g*-PEG concentration, given a constant starting PMAA

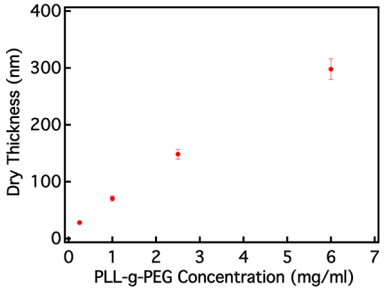

Figure 2. Dry thicknesses of PEC films with respect to different PLL-*g*-PEG concentrations in solution under constant adsorption conditions (adsorption time, 240 s; initial thickness of PMAA brushes, 22 nm; pH of HEPES buffer, 7.4).

thickness. A similar concentration-dependent adsorption behavior was also reported by Rühe[13,28] and Penn.[31]

In addition to the PLL-*g*-PEG concentration during adsorption, the influence of pH on the formation of PEC films was also investigated (Figure 3). When the adsorption

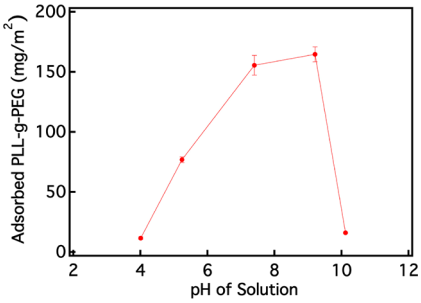

Figure 3. Adsorbed mass of PLL-*g*-PEG (2.5 mg/mL) at different pH values under constant adsorption conditions (incubating time, 240 s; initial thickness of PMAA brushes, 26 nm). Adsorbed amount (δ) of PLL-*g*-PEG is calculated according to the formula:[13] $\delta = \rho d'$, where ρ is the PLL-*g*-PEG density (1.27 g/cm^3) and d' is the change of (dry) thickness upon adsorption.

process was carried out at pH values lower than 4.0 or higher than 10, i.e. below and above the pK_as values of PMAA (4.66) and PLL (9.5),[32,33] respectively, no grafted PEC films were formed. Outside of the 4−10 pH range, either PMAA or PLL possessed no net charge, and thus the driving force leading to the formation of PECs was absent. Hence we believe that the very low residual adsorption observed under these conditions was solely due to the formation of hydrogen bonding between the PLL-*g*-PEG and PMAA. In contrast, PLL-*g*-PEG strongly adsorbs when the pH value of the incubation solution was set in between the pK_as of these polyacids and polybases, to form PEC films. The adsorbed copolymer mass increased monotonically above a pH value of 4.0 and reached a maximum between 7 and 9, evidencing the formation of PECs due to electrostatic interactions between the negatively charged PMAA brushes and the positively charged PLL backbones.

In addition to the influence of pH on the fabrication of PEC films, the ionic strength of the medium was varied, in order to study the influence of salt concentration on polyelectrolyte self-assembly. The presence of dissolved ions can significantly affect the swelling equilibrium of weak polyelectrolyte brushes;[34−36] therefore, the complexing process was conducted at different NaCl concentrations, as shown in Figure 4. When the concentration of NaCl in the aqueous medium is low, PMAA

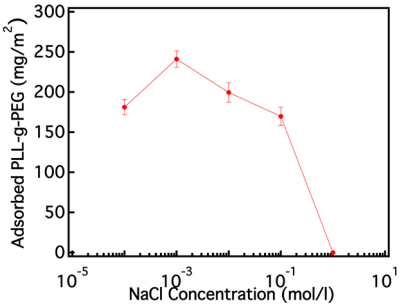

Figure 4. Adsorption of PLL-*g*-PEG at different salt concentrations under constant adsorption conditions (adsorption time, 240 s; initial thickness of PMAA brushes, 19 nm; PLL-*g*-PEG concentration, 2.5 mg/mL; pH of solution, 7.4).

brushes behave according to the "osmotic brush" regime.[13] In this situation, the presence of salt produces a shift in the dissociation equilibrium, favoring the formation of carboxylate moieties along the PMAA backbones. This phenomenon induces brush stretching and an increase in PLL-*g*-PEG adsorbed mass. The adsorbed mass of copolymer reaches a maximum at a specific NaCl concentration (1 mM) and further increase of salt concentration in the adsorbing solution caused the PMAA brushes to adopt the so-called "salted brush".[13] In this situation, dissolved ions screen the charges along the polyelectrolyte brush chains, inhibiting PMAA dissociation and reducing the driving force for complexation. This phenomenon hindered PLL-*g*-PEG adsorption until no observable PEC films were formed, as in the case of concentrated, 1 M NaCl solutions.

Interfacial Properties of Grafted PEC Films. The surface morphology of grafted PEC films was studied by tapping-mode AFM and the corresponding images are shown in Figures 5.

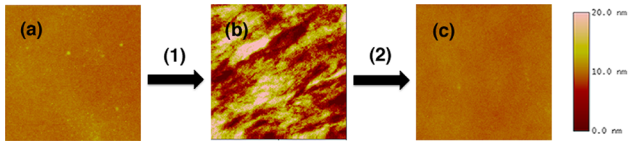

Figure 5. Dry morphology of (a) PMAA brushes with thickness of 33 nm and roughness (rms) of 0.4 nm, (b) PEC films with thickness of 426 nm and roughness (rms) of 4 nm, and (c) PMAA brushes with thickness of 31 nm and roughness (rms) of 0.4 nm after the desorption process (scanning size: 5 μm × 5 μm). (1) Adsorption of PLL-*g*-PEG, (2) desorption of PLL-*g*-PEG in NaCl solution (1 M).

PLL-*g*-PEG adsorption in PMAA causes an increase in RMS roughness on the polymer films, from (a) 0.4 ± 0.2 nm to (b) 4 ± 2 nm (measured over 5 μm × 5 μm). The increased roughness is attributed to the formation of PLL-*g*-PEG/PMAA aggregates in the grafted PEC films.

In order to confirm the reversibility of the complexation process of the copolymers, the PEC films were immersed in 1 M NaCl solution for 5 s and effective PEC dissolution was confirmed by AFM imaging. Uniformly smooth polymer films were obtained due to the salt-driven dissociation of PLL-*g*-PEG/PMAA complexes and the recovery of the original PMAA brushes.

The morphologies of grafted PEC films containing different masses of PLL-*g*-PEG with identical starting PMAA thickness are shown in Figure 6. Upon increasing the adsorbed amount of PLL-*g*-PEG, the roughness of the grafted PEC films was found

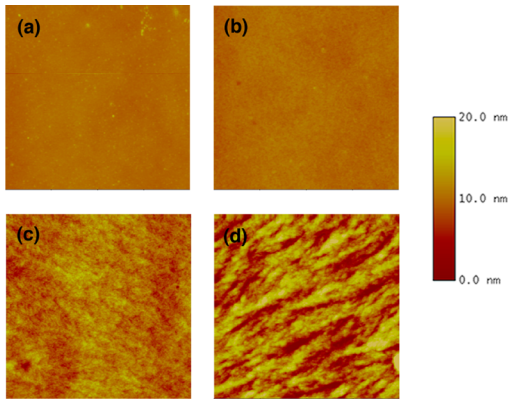

Figure 6. Dry morphology of PEC films (scanning size, 10 μm × 10 μm), fabricated by using identical PMAA brushes (initial dry thickness, 22 nm) and loading with PLL-*g*-PEG at different concentrations: (a) C = 0.25 mg/mL, (b) C = 1.0 mg/mL, (c) C = 2.5 mg/mL, and (d) C = 6.0 mg/mL for a constant adsorption time (240 s) (pH of solution, 7.4).

to increase. In particular, oriented morphologies on the surface of the PEC films were observed (Figure 6d) at high concentrations of adsorbed PLL-*g*-PEG. We believe that the observed morphology of PEC films in dry conditions is directly related to their conformation in swollen state. We thus presume that the oriented assemblies are caused by the adsorption of PLL-*g*-PEG along the highly extended grafted PMAA chains.

Stability of Grafted PEC Films. We examined the stability of the grafted PEC films in HEPES solution (1 mM) by monitoring the thickness variation as a function of incubation time. As can be seen in the Supporting Information, the dry thickness of the PMAA brushes decreased by 71% and 82% following 7 and 14 days of incubation, respectively. The dry thickness of the PLL-*g*-PEG films formed on SiOx surfaces decreased by 32% and 55% over the same incubation times.[37] In contrast, the overall thickness of grafted PEC films was shown to decrease by 15% after 1 week of incubation and by 35% after 2 weeks of incubation (see the Supporting Information). Thus the formation of PMAA/PLL-*g*-PEG complexes at the surface resulted in a significant enhancement of film stability when compared to the either singly (physically or chemically) grafted component.

Polyelectrolyte brushes, such as PMAA, have been observed to detach from the surface in an aqueous environment due to hydrolysis of the anchoring groups, and assisted by the relatively high osmotic pressure inside the brush structure and entropic effects.[38−40] Assembly of PECs induced a modification of PMAA conformation (vide infra) as well as a loss of net charge along the grafted backbones. We believe that both phenomena inhibit chain desorption, consequently increasing the film stability. This important finding additionally paves the way for possible future applications of grafted PECs as a platform in biological systems and biomaterials.

Structure of Grafted PEC Films Probed by Confocal Fluorescence Microscopy. To gain further insight into the mechanism of PLL-*g*-PEG adsorption into PMAA brushes and to visualize the structure of the subsequently assembled grafted PECs, we probed samples fabricated with fluorophore-labeled PLL-*g*-PEG (red and green) with confocal fluorescent microscopy. Fluorescence images recorded at different distances from the underlying silicon substrate were used to reconstruct the 3D distribution of PLL-*g*-PEG within the grafted PECs.

In Figure 7a, we show the 3D distribution of red fluorophore within grafted PEC films, swollen in water, following two hours

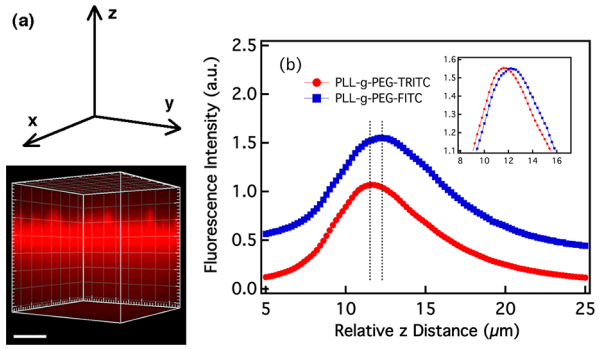

Figure 7. (a) Reconstruction of confocal data obtained for fluorescence-labeled PLL-*g*-PEG in swollen, saturated PEC films with a dry thickness of 592 nm and an initial PMAA dry thickness of 65 nm (scale bar, 10 μm; the silicon substrate lying in the x−y plane beneath the fluorescence-labeled layer). (b) Normalized fluorescence intensity distribution (y-shifted in inset for clarity) after loading PLL-*g*-PEG-FITC (green fluorescence, dry thickness: 157 nm) into swollen PEC films, preloaded (not saturated) with PLL-*g*-PEG-TRITC (red fluorescence; dry thickness, 111 nm) (dashed line indicates the position where maximum fluorescence intensity is reached; silicon substrate is at right side of the plot).

of adsorption of PLL-*g*-PEG-TRITC. The maximum fluorescence intensity was located at the interface between the film and the surrounding solution, gradually fading away at positions closer to the substrate. This finding demonstrates that PLL-*g*-PEG is intercalated inside the PMAA brushes in a decreasing concentration gradient toward the underlying substrate surface.

In Figure 7b, we show the fluorescence-intensity profile of the PMAA scaffolds in water, treated sequentially with PLL-*g*-PEG-TRITC and then PLL-*g*-PEG-FITC. Following adsorption of PLL-*g*-PEG-FTIC into PLL-*g*-PEG-TRITC-preloaded PEC films, the fluorescence intensity of both fluorophores was measured. The FITC intensity maximum was found to be shifted by 800 nm with respect to the TRITC maximum, in the direction of the silicon substrate. The fluorescence distribution is a convolution of the adsorption profile and the intrinsic profile of the confocal microscope.

The results obtained in these experiments confirmed that PLL-*g*-PEG adsorption kinetics was determined by the diffusion of the copolymers into the PMAA brushes. The PLL-*g*-PEG copolymers were concentrated at the brushes surface, since further diffusion inside PMAA scaffolds had to overcome both the steric hindrance by preadsorbed copolymers and the loss of net opposite charge due to PEC formation. Additional adsorption of the PLL-*g*-PEG on preformed, grafted PEC films showed a further diffusion of copolymers toward the underlying substrate.

Mechanical Properties of Grafted PEC Films. The mechanical properties of grafted PEC films were studied by AFM indentation under buffer solution and compared to the starting PMAA brushes. Upon adsorption of PLL-*g*-PEG, the PMAA films were shown to increase their Young's moduli from 0.4 ± 0.1 kPa to 1.3 ± 0.3 kPa, as indicated by the steepening of the indentation curve shown in Figure 8. Film stiffening upon PEC formation was because of filling of the brush films when

dx.doi.org/10.1021/am4006379 | ACS Appl. Mater. Interfaces 2013, 5, 4913−4920

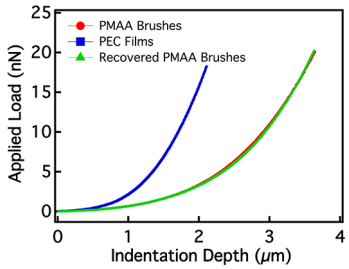

Figure 8. Indentation of PMAA brushes upon loading and unloading in HEPES buffer (only approaching curves are shown; dry thicknesses of PMAA brushes and PEC films are 22 and 148 nm, respectively; adsorbed mass of PLL-*g*-PEG, 160.02 mg/m^2), measured by colloidal probe microscopy with a gold-coated silica sphere (spring constant, 0.067 N/m; sphere radius, 10 μm).

oppositely charged PLL segments were complexed along the grafted PMAA chains. This is related to the formation of physical interactions (and potentially cross-linking) between PMAA chains and the PLL segments, which also leads to film shrinkage. It is worth mentioning that compared to covalently cross-linked films[25] the weak physical interactions in grafted PECs only induced limited stiffening with respect to the starting PMAA brushes. This is due to the high swelling of PEC films generated from weak polyelectrolyte complexes, distinguishing them from strong PECs.[41−43]

The stiffening effect caused by PEC formation was found to be completely reversible upon salt-induced desorption of PLL-*g*-PEG adsorbents. As can be seen in Figure 8, immersion of grafted PECs in 1 M NaCl solution for 5 s returned the Young's modulus (decrease of the indentation curve slope) to a value of 0.4 ± 0.1 kPa, which was characteristic of the starting PMAA brushes.

The stiffening of grafted PECs could be additionally monitored by AFM indentation as a function of the amount of PLL-*g*-PEG adsorbed into the PMAA brushes. Progressive loading of PLL-*g*-PEG caused both a shrinkage and a gradual increase of film stiffness, as shown in the indentation profiles reported in Figure 9. Typical Young's moduli thus ranged from 0.4 ± 0.1 kPa for the starting PMAA brushes to 0.7 ± 0.2 kPa, 1.3 ± 0.2 kPa and 1.6 ± 0.2 kPa following the adsorption of 83.8, 135.9, and 233.7 mg/m^2 PLL-*g*-PEG, respectively.

Nanotribological Properties of Grafted PEC films. Hydrophilic polymer brushes and polyelectrolyte brushes have been already reported to display highly lubricious behavior in aqueous environments.[44−46] For this reason, in addition to the mechanical characterization of grafted PEC films, we have also investigated the nanotribological properties of the synthesized films by means of colloidal probe microscopy in an aqueous environment. As shown in Figure 10, PMAA brushes showed a very low coefficient of friction (0.01), when slid against a gold-coated silica sphere, indicating very effective lubricating behavior. However, upon formation of the PEC films, the coefficient of friction (COF) increased to a value of 0.04. The 4-fold increase in COF was presumably due to the greater number of dissipative pathways upon complexation of PMAA brushes with PLL-*g*-PEG. A similar phenomenon has been already observed in covalently cross-linked brush systems on the same contact scale.[18]

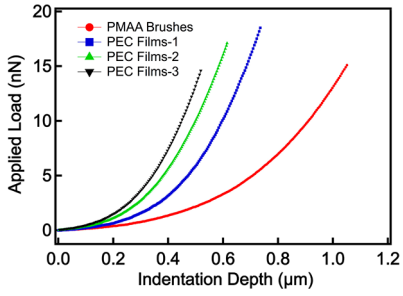

Figure 9. Indentation of PMAA brushes upon loading with different amounts of PLL-*g*-PEG in HEPES buffer (only approaching curves are shown, dry thicknesses of PMAA brushes and PEC films 1, 2, 3 are 18, 84, 125, and 202 nm, respectively), measured by colloidal probe microscopy with a gold-coated silica sphere (spring constant: 0.217 N/m, sphere radius: 8.5 μm).

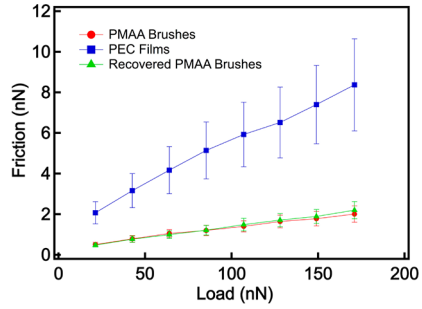

Figure 10. Friction of PMAA brushes as a function of load in HEPES buffer (dry thicknesses of PMAA and PEC films are 22 and 148 nm, respectively, adsorbed mass of PLL-*g*-PEG: 160.02 mg/m^2), measured by colloidal probe microscopy with a gold-coated silica sphere (spring constant: 0.067 N/m, sphere radius: 10 μm).

The lubrication properties of grafted PEC films could also be used to indicate the reversible loading of PLL-*g*-PEG and thus the restoring of the starting PMAA brush upon salt treatment. As is shown in Figure 10, incubation of grafted PEC films in 1 M NaCl led to PLL-*g*-PEG desorption and the friction behavior of the films showed the regeneration of the original PMAA brushes.

Progressive adsorption of PLL-*g*-PEG into PMAA brushes is able to gradually increase the stiffening of the swollen brushes and therefore leads to an increase of COF for the generated PEC films, as shown in Figure 11. The COF values increased from 0.01 of the starting PMAA brushes to 0.03, 0.04, and 0.06 following the adsorption of 45.7, 140.9, and 820.4 mg/m^2 PLL-*g*-PEG, respectively.

Since PLL-*g*-PEG is known to function as a lubricious coating on flat surfaces, such as silicon oxide,[17] one might expect that the adsorption of these macromolecules into PMAA brushes would lead to low friction. As this is apparently not the case, we can conclude that the PEG moieties of the PLL-*g*-PEG are held within the PMAA scaffolds, and are not present to a significant extent on the outer, sliding surface of the grafted PECs.

CONCLUSION

We have reported the synthesis and characterization of grafted polyelectrolyte complex films, employing a combination of both "grafting-from" and "grafting-to" strategies, i.e., electrostatically adsorbing PLL-*g*-PEG copolymers to oppositely charged, surface-tethered PMAA brushes. The grafting kinetics of PEC films could be tailored in a controlled fashion by tuning the adsorption time, starting PMAA-brush thickness, PLL-*g*-PEG

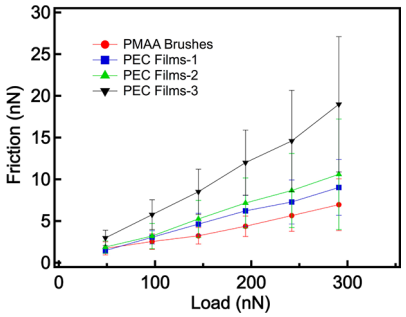

Figure 11. Friction of PMAA brushes and PEC films with different uptakes of PLL-*g*-PEG in HEPES buffer (dry thicknesses of PMAA brushes and PEC films 1, 2, 3 are 40, 76, 151, and 686 nm, respectively), measured by colloidal-probe microscopy with a gold-coated silica sphere (spring constant, 0.5078 N/m; sphere radius, 8.66 μm).

concentration in solution, pH and salt concentration of the solution. The grafted PEC films showed enhanced stability compared to those of the individual grafted components. Furthermore, the distribution of PLL-*g*-PEG copolymers in PEC films was determined optically, in order to understand the structure of the films in their swollen state. The high mass/charge ratio that characterizes PLL-g-PEG causes an amplification of the filling effect when fabricating PECs, which leads to the approximate retention of the swollen dimensions of the PMAA brushes, even in the dry state. Finally, mechanical and nanotribological properties of these PEC films were studied by using colloidal-probe microscopy in aqueous phase. The PEC films presented tunable mechanical behavior, and provide potential building blocks for application in a wide variety of technologies.

■ ASSOCIATED CONTENT

Supporting Information

Details of FT-IR spectra of PMAA brushes and grafted polyelectrolyte complex films and stability of PMAA brushes and grafted PEC films in HEPES buffer. This material is available free of charge via the Internet at http://pubs.acs.org.

■ AUTHOR INFORMATION

Corresponding Author

* E-mail: nspencer@ethz.ch. Fax: +41-44-6331027. Tel: +41-44-6325850.

Notes

The authors declare no competing financial interest.

■ ACKNOWLEDGMENTS

The financial assistance of the European Science Foundation through their Eurocores (FANAS) program is gratefully acknowledged. Dr. Gábor Csúcs (Light Microscopy and Screening Center, ETH Zurich, Switzerland) is thanked for allowing access to confocal fluorescence microscopy. The authors also thank Dr. Prathima C. Nalam (Department of Mechanical Engineering and Applied Mechanics, University of Pennsylvania) for fruitful discussions and suggestions.

■ REFERENCES

(1) Barbey, R.; Lavanant, L.; Paripovic, D.; Schüwer, N.; Sugnaux, C.; Tugulu, S.; Klok, H. A. *Chem. Rev.* **2009**, *109*, 5437−5527.
(2) Zhao, B.; Brittain, W. J. *Prog. Polym. Sci.* **2000**, *25*, 677−710.
(3) Ejaz, M.; Yamamoto, S.; Ohno, K.; Tsujii, Y.; Fukuda, T. *Macromolecules* **1998**, *31*, 5934−5936.
(4) Kenausis, G. L.; Vörös, J.; Elbert, D. L.; Huang, N. P.; Hofer, R.; Ruiz-Taylor, L.; Textor, M.; Hubbell, J. A.; Spencer, N. D. *J. Phys. Chem. B* **2000**, *104*, 3298−3309.
(5) Pasche, S.; De Paul, S. M.; Vörös, J.; Spencer, N. D.; Textor, M. *Langmuir* **2003**, *19*, 9216−9225.
(6) Toomey, R.; Freidank, D.; Rühe, J. *Macromolecules* **2004**, *37*, 882−887.
(7) Decher, G. *Science* **1997**, *277*, 1232−1237.
(8) Dautzenberg, H.; Karibyants, N.; Zaitsev, S. Y. *Macromol. Rapid Commun.* **1997**, *18*, 175−182.
(9) Wolfert, M. A.; Dash, P. R.; Navarova, O.; Oupicky, D.; Seymour, L. W.; Smart, S.; Strohalm, J.; Ulbrich, K. M. A. *Bioconjugate Chem.* **1999**, *10*, 993−1004.
(10) Ma, Y. J.; Dong, W. F.; Hempenius, M. A.; Möhwald, H.; Vancso, G. J. *Nat. Mater.* **2006**, *5*, 724−729.
(11) Elbert, D. L.; Herbert, C. B.; Hubbell, J. A. *Langmuir* **1999**, *15*, 5355−5362.
(12) Thünemann, A. F.; Müller, M.; Dautzenberg, H.; Joanny, J. F. O.; Löwen, H. *Adv. Polym. Sci.* **2004**, *166*, 113−171.
(13) Zhang, H. N.; Rühe, J. *Macromolecules* **2005**, *38*, 10743−10749.
(14) Llarena, I.; Iturri Ramos, J. J.; Donath, E.; Moya, S. E. *Macromol. Rapid Commun.* **2010**, *31*, 526−531.
(15) Laurent, P.; Souharce, G.; Duchet-Rumeau, J.; Portinha, D.; Charlot, A. *Soft Matter* **2012**, *8*, 715−725.
(16) Huang, N. P.; Vörös, J.; De Paul, S. M.; Textor, M.; Spencer, N. D. *Langmuir* **2002**, *18*, 220−230.
(17) Müller, M. T.; Yan, X.; Lee, S.; Perry, S. S.; Spencer, N. D. *Macromolecules* **2005**, *38*, 3861−3866.
(18) Li, A.; Ramakrishna, S. N.; Kooij, E. S.; Espinosa-Marzal, R. M.; Spencer, N. D. *Soft Matter* **2012**, *8*, 9092−9100.
(19) Butt, H. J.; Jaschke, M. *Nanotechnology* **1995**, *6*, 1−7.
(20) Green, C. P.; Lioe, H.; Cleveland, J. P.; Proksch, R.; Mulvaney, P.; Sader, J. E. *Rev. Sci. Instrum.* **2004**, *75*, 1988−1996.
(21) Ducker, W. A.; Senden, T. J.; Pashley, R. M. *Nature* **1991**, *353*, 239−241.
(22) Cannara, R. J.; Eglin, M.; Carpick, R. W. *Rev. Sci. Instrum.* **2006**, *77*, 053701−1−053701−11.
(23) Sui, X. F.; Chen, Q.; Hempenius, M. A.; Vancso, G. J. *Small* **2011**, *7*, 1440−1447.
(24) Olanya, G.; Iruthayaraj, J.; Poptoshev, E.; Makuska, R.; Vareikis, A.; Claesson, P. M. *Langmuir* **2008**, *24*, 5341−5349.
(25) Li, A.; Benetti, E. M.; Tranchida, D.; Clasohm, J. N.; Schönherr, H.; Spencer, N. D. *Macromolecules* **2011**, *44*, 5344−5351.
(26) de Vos, W. M.; Kleijn, J. M.; de Keizer, A.; Cohen Stuart, M. A. *Angew. Chem., Int. Ed.* **2009**, *48*, 5369−5371.
(27) Feuz, L. *Ph.D. Thesis*, Department of Materials, ETH Zurich, Zurich, Switzerland, 2006.
(28) Schuh, C.; Rühe, J. *Macromolecules* **2011**, *44*, 3502−3510.
(29) Schüwer, N.; Klok, H. A. *Langmuir* **2011**, *27*, 4789−4796.
(30) Huang, N. P.; Michel, R.; Vörös, J.; Textor, M.; Hofer, R.; Rossi, A.; Elbert, D. L.; Hubbell, J. A.; Spencer, N. D. *Langmuir* **2001**, *17*, 489−498.
(31) Huang, H. Q.; Cammers, A.; Penn, L. S. *Macromolecules* **2006**, *39*, 7064−7070.
(32) Mark, J. E. *Polymer Data Handbook*; Oxford University Press: New York, 1999; pp 638−640.
(33) Franzin, C. M.; Macdonald, P. M. *Biophys. J.* **2001**, *81*, 3346−3362.
(34) Biesalski, M.; Johannsmann, D.; Rühe, J. *J. Chem. Phys.* **2002**, *117*, 4988−4994.
(35) Rühe, J.; Ballauff, M.; Biesalski, M.; Dziezok, P.; Grohn, F.; Johannsmann, D.; Houbenov, N.; Hugenberg, N.; Konradi, R.; Minko, S.; Motornov, M.; Netz, R. R.; Schmidt, M.; Seidel, C.; Stamm, M.; Stephan, T.; Usov, D.; Zhang, H. N. *Adv. Polym. Sci.* **2004**, *165*, 79−150.
(36) Zhulina, E. B.; Birshtein, T. M.; Borisov, O. V. *Macromolecules* **1995**, *28*, 1491−1499.

(37) Konradi, R.; Acikgoz, C.; Textor, M. *Macromol. Rapid Commun.* **2012**, *33*, 1663−1676.
(38) Zhang, Y. X.; He, J. A.; Zhu, Y.; Chen, H.; Ma, H. W. *Chem. Commun.* **2011**, *47*, 1190−1192.
(39) Lego, B.; Skene, W. G.; Giasson, S. *Macromolecules* **2010**, *43*, 4384−4393.
(40) Paripovic, D.; Klok, H. A. *Macromol. Chem. Phys.* **2011**, *212*, 950−958.
(41) Ellipsometry in liquid experiments was also conducted; however, PECs films were strongly swollen in water and no refractive index contrast between polymer films and water was detected. Therefore, swelling thicknesses of these films were not able to be obtained by ellipsometry.
(42) Zhang, H. N.; Rühe, J. *Macromolecules* **2003**, *36*, 6593−6598.
(43) Zhang, H. N.; Rühe, J. *Macromol. Rapid Commun.* **2003**, *24*, 576−579.
(44) Kobayashi, M.; Takahara, A. *Chem. Rec.* **2010**, *10*, 208−216.
(45) Lee, S.; Spencer, N. D. *Science* **2008**, *319*, 575−576.
(46) Chen, M.; Briscoe, W. H.; Armes, S. P.; Klein, J. *Science* **2009**, *323*, 1698−1701.